ACS APPLIED MATERIALS & INTERFACES

Letter

www.acsami.org

In Situ Analysis of Gas Generation in Lithium-Ion Batteries with Different Carbonate-Based Electrolytes

Xin Teng,[†] Chun Zhan,[‡] Ying Bai,[*,†] Lu Ma,[§] Qi Liu,[†] Chuan Wu,[†,∥] Feng Wu,[†,∥] Yusheng Yang,[†] Jun Lu,[*,‡] and Khalil Amine[‡]

[†]Beijing Key Laboratory of Environment Science and Engineering, School of Materials Science and Engineering, Beijing Institute of Technology, Beijing 100081, China

[‡]Chemical Sciences and Engineering Division and [§]Advanced Photon Sources, X-ray Science Division, Argonne National Laboratory, 9700 South Cass Avenue, Lemont, Illinois 60439, United States

[∥]Collaborative Innovation Center of Electric Vehicles in Beijing, Beijing 100081, China

Supporting Information

ABSTRACT: Gas generation in lithium-ion batteries is one of the critical issues limiting their safety performance and lifetime. In this work, a set of 900 mAh pouch cells were applied to systematically compare the composition of gases generated from a serial of carbonate-based composite electrolytes, using a self-designed gas analyzing system. Among electrolytes used in this work, the composite γ-butyrolactone/ethyl methyl carbonate (GBL/EMC) exhibited remarkably less gassing because of the electrochemical stability of the GBL, which makes it a promising electrolyte for battery with advanced safety and lifetime.

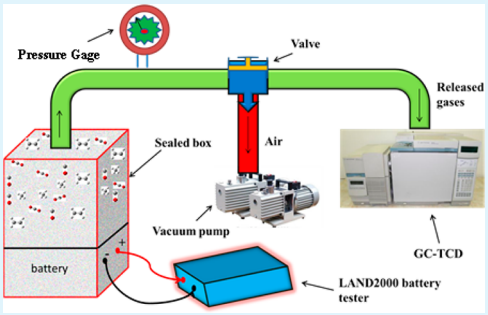

KEYWORDS: *lithium ion battery, carbonate electrolytes, gas generation, pouch cells, density function theory*

Currently, lithium-ion batteries (LIBs) have been widely used in portable electronics and power tools due to its high energy density.[1−10] Despite the major advances over the last few decades, gas generation during the formation, operation, and storage of the LIBs remains a big challenge, because of the concomitant volume swelling, performance failure, and safety concerns.[11−14] Gas generation in the formation step of the batteries is mainly originated from the electrochemical decomposition of electrolyte solvents during the solid-electrolyte interphase (SEI) layer formation,[15−21] which requires an extra degassing process, especially for the "soft" pouch cells, and thus increases the production cost and potentially degrades the consistency of cell groups. Comparatively, gas releasing during cycling and storage of well-formed cells is generally less severe if no abuse condition such as overcharging or overheating is applied. That is because the as-formed SEI layer is able to reduce direct contact between the electrode and the electrolytes.

Because of their scaled-up, automotive fabrication process and the sufficient amount of active materials and electrolyte, the pouch cells designed for practical application are able to provide more reliable insights of the gassing process compared to lab-scale coin cells. In this work, a set of 900 mAh commercial pouch cells were assembled to analyze the gas composition at a series of state of charge (SOC) in the first formation cycle of the cells. A set of different carbonate composite electrolytes were applied to compare the gaseous products generated by decomposition of different solvents. It was found that low-molecular-weight hydrocarbons such as CH_4, C_2H_4, and C_2H_6, and carbon oxides such as CO and CO_2 were the main gaseous during the initial charging of the battery. Among electrolytes used in this work, the composite γ-butyrolactone/ethyl methyl carbonate (GBL/EMC) exhibited remarkably less gassing due to the electrochemical stability of the GBL, which makes it a promising electrolyte for battery with advanced safety and lifetime.

Using the typical commercial LIB configuration, the pouch cells for gas analysis were assembled with $LiCoO_2$ as the cathode material and the nature graphite as the anode material. The electrolytes are consisted of 1 M $LiPF_6$ dissolved in binary carbonate solvents including EC (ethylene carbonate), FEC (fluoroethylene carbonate), GBL (γ-butyrolactone), DMC (dimethyl-carbonate), EMC (ethyl methyl carbonate), and DEC (diethyl carbonate), with their detailed composition and volume ratio listed in Table S1. The cells were first placed in a sealed gas analysis system as shown in the TOC graphic, and then charged at 0.5C to reach a series of different SOC, i.e., 5, 10, 20, 30, 50, and 100%. The gas inside the cell was released by nailing the cells at the same spot, and its composition was analyzed by a gas chromatography analysis and thermal conductivity detector (GC-TCD). The gas analysis system is

Received: September 7, 2015
Accepted: September 29, 2015
Published: September 29, 2015

DOI: 10.1021/acsami.5b08399
ACS Appl. Mater. Interfaces 2015, 7, 22751−22755

shown in Scheme 1, and more experimental details can be found in the Supporting Information.

Scheme 1. Gas Analysis System for Lithium Ion Batteries

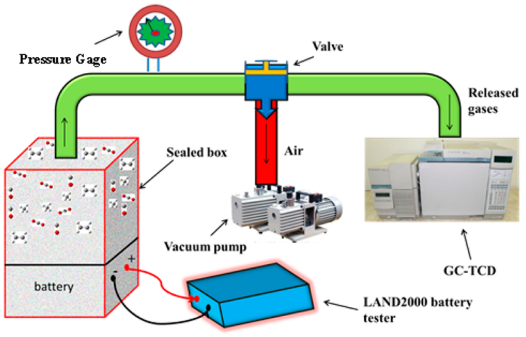

The gas composition of cells with EC-containing electrolytes (No. 1, 2, and 3) are plotted in Figure 1. It is notable that C_2H_4 and CO are the major gas products from all of the EC-containing electrolytes. The reductive decomposition reactions of EC generating C_2H_4 and CO can be expressed by eqs 1 and 2 in Scheme 2.

In the cell with EC/EMC solvent (Figure 1a), the volumes of the main gas products decrease with higher SOC, indicating that the two gases may be dissolved or reacted with other component in the batteries during the process of charging.[22] Then EMC is replaced by DMC, the volume of CO and C_2H_4 increase in the beginning when SOC is lower than 10%, indicating a relatively slower decomposition reaction. On the other hand, the volumes of the minority gases such as CH_4, C_2H_6, and CO_2 increase with higher SOC, showing that these gases accumulate gradually in the cell, whereas the electrochemical reactions of the linear carbonates (such as the one shown in eq 3 in Scheme 2) undergoing. Furthermore, it is interesting that in Figure 1, there are CO_2 generated from EMC and DEC, but not DMC. Therefore, the CO_2 is likely originated from the existence of the ethyl group.

Scheme 2

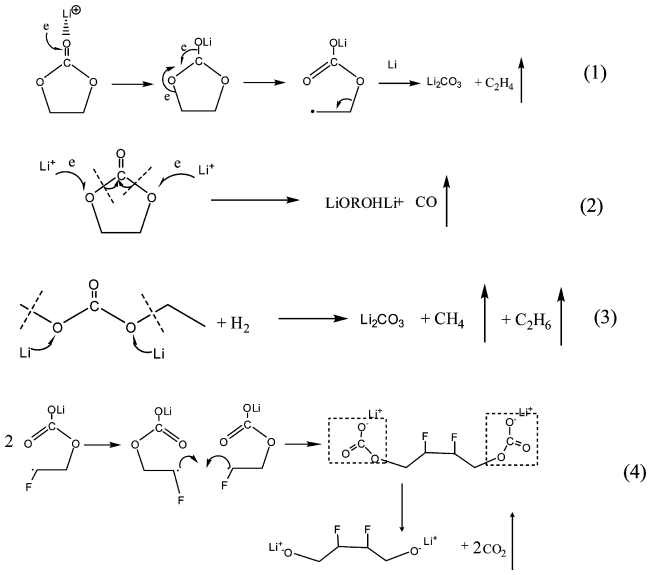

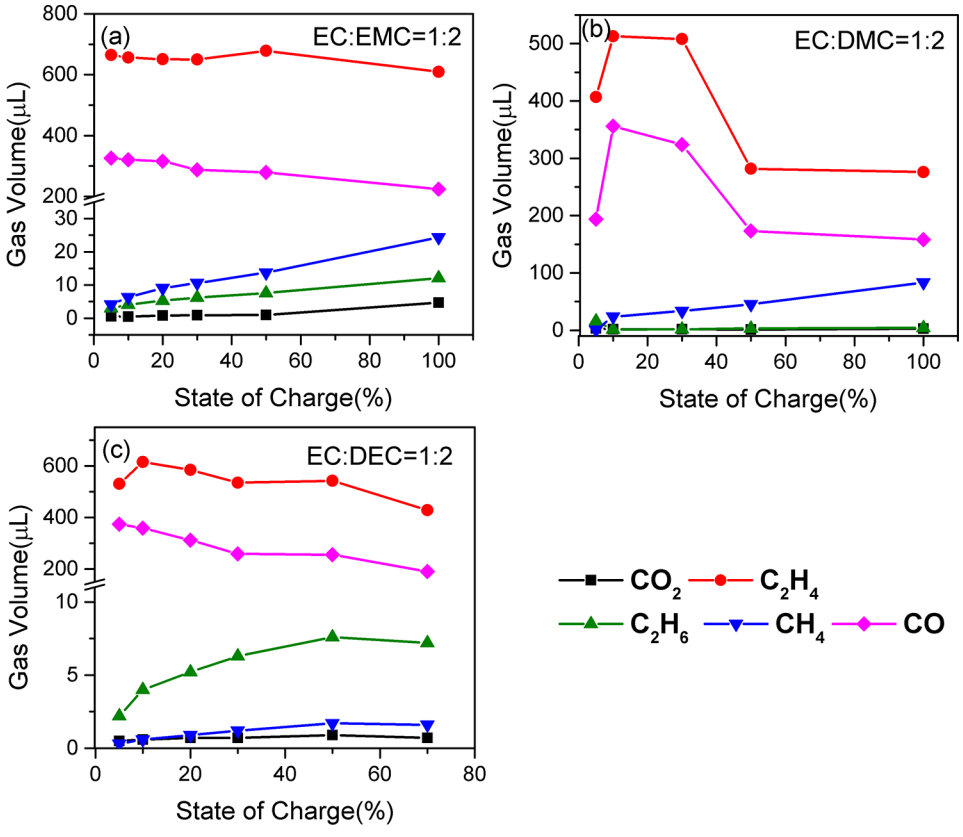

Figure 1. Compositions of gas generated at different SOC in the first charge of cells using EC-containing electrolytes. (a) EC:EMC = 1:2, (b) EC:DMC = 1:2, (c) EC:DEC = 1:2.

DOI: 10.1021/acsami.5b08399
ACS Appl. Mater. Interfaces 2015, 7, 22751−22755

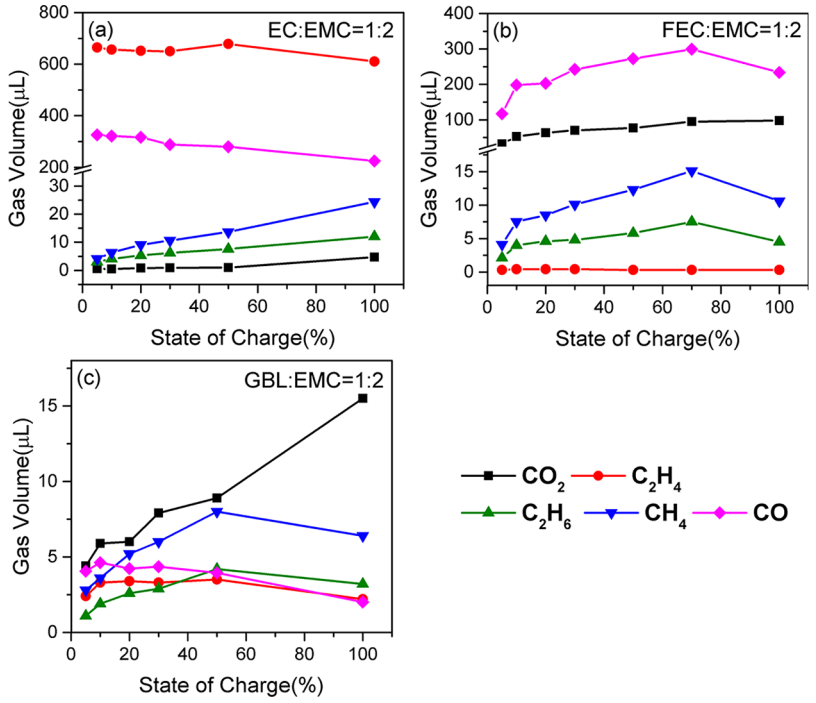

Figure 2. Compositions of gas generated at different SOC in the first charge of cells using EMC-containing electrolytes. (a) EC:EMC = 1:2, (b) FEC: EMC = 1:2, (c) GBL:EMC = 1:2.

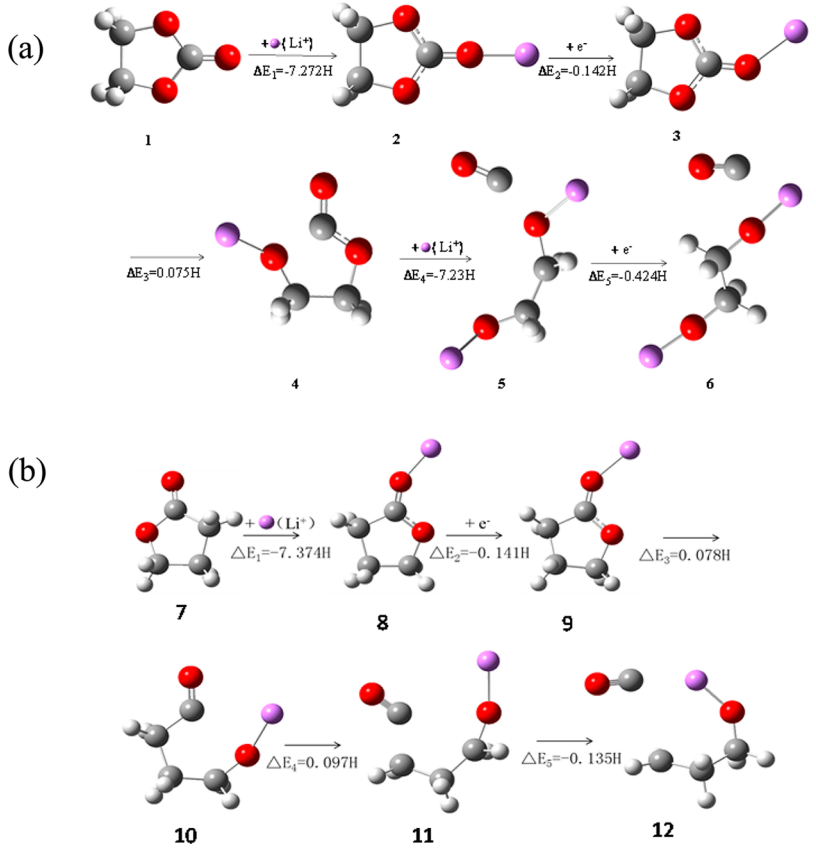

Figure 3. Energy profile at 298.15 K of the reductive dissociation process of (a) EC and (b) GBL. The gray, white, red, and purple balls stand for C, H, O, and Li atoms, respectively.

To further understand the generation of the main gas composition from the EC-containing electrolytes, we used GBL and FEC instead of EC, and their gas generations are compared in Figure 2. The content of C_2H_4 dropped significantly in the absence of EC, further confirming that C_2H_4 is the mainly originated from the decomposition of EC. The FEC:EMC

DOI: 10.1021/acsami.5b08399
ACS Appl. Mater. Interfaces 2015, 7, 22751−22755

electrolyte still released about 250 μL of CO because of the similarity in the ring carbonate structure of EC and FEC. Meanwhile, moderate amounts of CO_2 can be detected, and the reaction path can be expressed as eq 4 in Scheme 2.

The structure of FEC is very similar to that of EC. The only difference is a fluoride in FEC replacing for the hydrogen in EC molecule. When Li^+ combines with FEC, the C−F bond is open and the electron transfer goes on. The radical anion intermediate is unstable and tends to terminate by dimerization. The dotted-line parts in the dimer have strong ion properties that are similar to those of carbonate and can be further decomposed to CO_2.

As shown in Figure 2c, when the EC is replaced by GBL, the electrolyte exhibits a much lower volume of CO and C_2H_4. To elucidate the remarkably reduced gassing in the GBL electrolyte compared to the EC electrolyte, we compared the reductive decompositions of EC and GBL by means of density functional theory calculation. As shown in Figure 3a, EC initially turns into the ion pair intermediate product (2), when a Li^+ tends to coordinate with the most electronegative O atom. The interaction energy, defined as the energy difference between the Li^+-EC and the total of Li^+ and the EC molecular, is about −7.272H, indicating a strong interaction between Li^+ and EC. Then an electron transfers from anode to further stabilize the intermediate product (2) to form the intermediate product (3). After that, about 0.0075H energy barrier exits to break the C−O bond and open the ring to from intermediate products (4). With the presence of another Li^+ and electron, the intermediate product (4) is eventually dissociated in to $LiOCH_2OLi$ and CO. Compared to EC, the GBL exhibits similar reaction path and energetic data in the reaction with the first Li^+ and electron to form the open-circuit intermediate (10). However, an energy barrier of about 0.0097H exits to break the C−C in intermediate (10) for further dissociation, because of the lack of anther C−O single bond to host the second Li^+ ion to push the relocation of electrons. Therefore, the energy barrier for the decomposition of Li^+(GBL) intermediate inhibits the gas generation from GBL: EMC electrolyte.

In summary, the mechanism of gas generation in the first charging process of lithium-ion batteries was investigated by experimental and theoretical analysis. The large amounts of C_2H_4 and CO generated from EC decomposition are the main gas product in the EC-containing electrolytes. The GBL/bEMC electrolyte exhibits much lower volume of gases compared to the EC or FEC-containing electrolytes, which was explained by DFT calculation. Therefore, it is promising for GBL/EMC solvent, which can efficiently suppress the generation of low-molecular-weight hydrocarbons and carbon oxides, to enhance the safety and electrochemical performance of the lithium-ion batteries.

■ ASSOCIATED CONTENT

Supporting Information

The Supporting Information is available free of charge on the ACS Publications website at DOI: 10.1021/acsami.5b08399.

Experimental details, battery assembling, gas composition analysis, and density functional theory (DFT) calculation, Table S1 (PDF)

■ AUTHOR INFORMATION

Corresponding Authors

*E-mail: membrane@bit.edu.cn. Tel:+86 10 68912528.

*E-mail: junlu@anl.gov. Tel.: +1 630-252-4485.

Notes

The authors declare no competing financial interest.

■ ACKNOWLEDGMENTS

This work is supported by the National Basic Research Program of China (2015CB251100), the Program for New Century Excellent Talents in University (NCET-13-0033), and the Beijing Co-construction Project (20150939014). The authors acknowledge Bryan Wood and Brian Way in BAK Canada for their support in gas components detection. Y.B. acknowledges the support from the State Scholarship Fund (201406035025) of the China Scholarship Council. C.Z., J.L., and K.A. were supported by the Center for Electrical Energy Storage, an Energy Frontier Research Center funded by the U.S. Department of Energy, Office of Science, Office of Basic Energy Sciences.

■ REFERENCES

(1) Goodenough, J. B.; Kim, Y. Challenges for Rechargeable Li Batteries. *Chem. Mater.* **2010**, *22*, 587−603.

(2) Armand, M.; Tarascon, J. M. Building Better Batteries. *Nature* **2008**, *451*, 652−657.

(3) Bai, Y.; Li, Y.; Wu, C.; Lu, J.; Li, H.; Liu, Z. L.; Zhong, Y. X.; Chen, S.; Zhang, C. Z.; Amine, K.; Wu, F. Lithium-Rich Nanoscale $Li_{1.2}Mn_{0.54}Ni_{0.13}Co_{0.13}O_2$ Cathode Material Prepared by Co-Precipitation Combined Freeze Drying (CP−FD) for Lithium-Ion Batteries. *Energy Technol.* **2015**, *3*, 843−850.

(4) Xu, K. Electrolytes and Interphases in Li-Ion Batteries and Beyond. *Chem. Rev.* **2014**, *114*, 11503−11618.

(5) Goodenough, J. B.; Park, K. S. The Li-Ion Rechargeable Battery: A Perspective. *J. Am. Chem. Soc.* **2013**, *135*, 1167−1176.

(6) Chen, Y.; Li, X.; Park, K.; Song, J.; Hong, J.; Zhou, L.; Mai, Y. W.; Huang, H.; Goodenough, J. B. Hollow Carbon-Nanotube/Carbon-Nanofiber Hybrid Anodes for Li-Ion Batteries. *J. Am. Chem. Soc.* **2013**, *135*, 16280−16283.

(7) Esbenshade, J. L.; Gewirth, A. A. Effect of Mn and Cu Addition on Lithiation and SEI Formation on Model Anode Electrodes. *J. Electrochem. Soc.* **2014**, *161*, A513−A518.

(8) Ziv, B.; Levy, N.; Borgel, V.; Li, Z.; Levi, M. D.; Aurbach, D.; Pauric, A. D.; Goward, G. R.; Fuller, T. J.; Balogh, M. P.; Halalay, I. C. Manganese Sequestration and Li-Ion Batteries Durability Enhancement by Polymeric 18-Crown-6 Ethers. *J. Electrochem. Soc.* **2014**, *161*, A1213−A1217.

(9) Chrétien, F.; Jones, J.; Damas, C.; Lemordant, D.; Willmann, P.; Anouti, M. Impact of Solid Electrolyte Interphase Lithium Salts on Cycling Ability of Li-ion Battery: Beneficial Effect of Glymes Additives. *J. Power Sources* **2014**, *248*, 969−977.

(10) Wu, F.; Wang, F.; Wu, C.; Bai, Y. Rate Performance of $Li_3V_2(PO_4)_3$/C Cathode Material and Its Li^+ Ion Intercalation Behavior. *J. Alloys Compd.* **2012**, *513*, 236−241.

(11) Kim, Y.; Jeong, D. Y.; Han, S. C. First-Principles Investigation of the Gas Evolution from the Cathodes of Lithium-Ion Batteries During the Storage Test. *J. Mater. Sci.* **2014**, *49*, 8444−8448.

(12) Xiao, L. F.; Ai, X. P.; Cao, Y. L.; Yang, H. X. Electrochemical Behavior of Biphenyl as Polymerizable Additive for Overcharge Protection of Lithium Ion Batteries. *Electrochim. Acta* **2004**, *49*, 4189−4196.

(13) Yoshida, H.; Fukunaga, T.; Hazama, T.; Terasaki, M.; Mizutani, M.; Yamachi, M. Degradation Mechanism of Alkyl Carbonate Solvents Used in Lithium-Ion Cells During Initial Charging. *J. Power Sources* **1997**, *68*, 311−315.

(14) Zhuang, G. V.; Yang, H.; Blizanac, B.; Ross, P. N. A study of Electrochemical Reduction of Ethylene and Propylene Carbonate Electrolytes on Graphite Using ATR-FTIR Spectroscopy. *Electrochem. Solid-State Lett.* **2005**, *8*, A441−A445.

DOI: 10.1021/acsami.5b08399
ACS Appl. Mater. Interfaces 2015, 7, 22751−22755

(15) Novák, P.; Panitz, J. C.; Joho, F. Advanced In Situ Methods for the Characterization of Practical Electrodes in Lithium-Ion Batteries. *J. Power Sources* **2000**, *90*, 52−58.
(16) Panitz, J. C.; Joho, F.; Novák, P. In Situ Characterization of a Graphite Electrode in a Secondary Lithium-Ion Battery Using Raman Microscopy. *Appl. Spectrosc.* **1999**, *53*, 1188−1199.
(17) Nie, M.; Chalasani, D.; Abraham, D. P.; Chen, Y.; Bose, A.; Lucht, B. L. Lithium Ion Battery Graphite Solid Electrolyte Interphase Revealed by Microscopy and Spectroscopy. *J. Phys. Chem. C* **2013**, *117*, 1257−1267.
(18) Nie, M.; Abraham, D. P.; Chen, Y.; Bose, A.; Lucht, B. L.Silicon Solid Electrolyte Interphase (SEI) of Lithium Ion Battery Characterized by Microscopy and Spectroscopy. *J. Phys. Chem. C* **2013**, *117*, 13403−13412.
(19) Zhao, H.; Park, S. J.; Shi, F.; Fu, Y.; Battaglia, V.; Ross, P. N.; Liu, G. Propylene Carbonate (PC)-Based Electrolytes with High Coulombic Efficiency for Lithium-Ion Batteries. *J. Electrochem. Soc.* **2014**, *161*, A194−A200.
(20) Shin, H.; Park, J.; Han, S.; Sastry, A. M.; Lu, W. Component-/Structure-Dependent Elasticity of Solid Electrolyte Interphase Layer in Li-Ion Batteries: Experimental and Computational Studies. *J. Power Sources* **2015**, *277*, 169−179.
(21) Serizawa, N.; Seki, S.; Takei, K.; Miyashiro, H.; Yoshida, K.; Ueno, K.; Tachikawa, N.; Dokko, K.; Katayama, Y.; Watanabe, M.; Miura, T. EQCM Measurement of Deposition and Dissolution of Lithium in Glyme-Li Salt Molten Complex. J. *J. Electrochem. Soc.* **2013**, *160*, A1529−A1533.
(22) Self, J.; Aiken, C. P.; Petibon, R.; Dahn, J. R. Survey of Gas Expansion in Li-Ion NMC Pouch Cells. *J. Electrochem. Soc.* **2015**, *162*, A796−A802.

DOI: 10.1021/acsami.5b08399
ACS Appl. Mater. Interfaces 2015, 7, 22751−22755